Title
H-Ras Transformation of Mammary Epithelial Cells Induces ERK-Mediated Spreading on Low Stiffness Matrix

Journal
Advanced Healthcare Materials, 9(8)

ISSN
2192-2640

Authors
Plunkett, Christopher
Kumar, Aditya
Yrastorza, Jaime
et al.

Publication Date
2020-04-01

DOI
10.1002/adhm.201901366

Peer reviewed

ADVANCED HEALTHCARE MATERIALS

Postfach 10 11 61
69451 Weinheim
Germany
Courier services:
Boschstraße 12
69469 Weinheim
Germany
Tel.: (+49) 6201 606 235
Fax: (+49) 6201 606 500
E-mail: advhealthmat@wiley.com

WILEY-VCH

Dear Author,

Please correct your galley proofs carefully and return them no more than four days after the page proofs have been received.

Please limit corrections to errors already in the text; cost incurred for any further changes or additions will be charged to the author, unless such changes have been agreed upon by the editor.

The editors reserve the right to publish your article without your corrections if the proofs do not arrive in time.

Note that the author is liable for damages arising from incorrect statements, including misprints.

Please note any queries that require your attention. These are indicated with a Q in the PDF and a question at the end of the document.

Reprints may be ordered by filling out the accompanying form.

Return the reprint order form by fax or by e-mail with the corrected proofs, to Wiley-VCH : advhealthmat@wiley.com

To avoid commonly occurring errors, **please ensure that the following important items are correct** in your proofs (please note that once your article is published online, no further corrections can be made):

- **Names** of all authors present and spelled correctly
- **Titles** of authors correct (Prof. or Dr. only: please note, Prof. Dr. is not used in the journals)
- **Addresses** and **postcodes** correct
- **E-mail address** of corresponding author correct (current email address)
- **Funding bodies** included and grant numbers accurate
- **Title** of article OK
- All **figures** included
- **Equations** correct (symbols and sub/superscripts)

Corrections should be made directly in the PDF file using the PDF annotation tools. If you have questions about this, please contact the editorial office. The corrected PDF and any accompanying files should be uploaded to the journal's Editorial Manager site.

Author Query Form

WILEY

Journal ADHM

Article adhm201901366

Dear Author,

During the copyediting of your manuscript the following queries arose.

Please refer to the query reference callout numbers in the page proofs and respond to each by marking the necessary comments using the PDF annotation tools.

Please remember illegible or unclear comments and corrections may delay publication.

Many thanks for your assistance.

Query No.	Description	Remarks
Q-OO	Open access publication of this work is possible via Wiley OnlineOpen. Information about this is available at: https://authorservices.wiley.com/author-resources/Journal-Authors/licensing-open-access/open-access/onlineopen.html. The cost of publishing your manuscript OnlineOpen may be covered by one of Wiley's national agreements. To find out more, visit https://authorservices.wiley.com/author-resources/Journal-Authors/open-access/affiliation-policies-payments/index.html. Note that eligibility for fee coverage is determined by the affiliation of the primary corresponding author designated at submission. Please log in to your Wiley Author Services account at https://authorservices.wiley.com/ and confirm your affiliation to see if you are eligible. Instructions for placing an OnlineOpen order can be found at: https://authorservices.wiley.com/author-resources/Journal-Authors/open-access/how-to-order-onlineopen.html. To publish your article open access, please complete the order process before completing your proof corrections.	
Q1	Please confirm that forenames/given names (blue) and surnames/family names (vermilion) have been identified correctly.	
Q2	Please provide the highest academic title (either Dr. or Prof.) for all authors, where applicable.	
Q3	Please define 'HEPES', 'DMEM', 'EDTA', 'MES', 'SDS' at their first occurrence in the text.	

Please confirm that Funding Information has been identified correctly.

Please confirm that the funding sponsor list below was correctly extracted from your article: that it includes all funders and that the text has been matched to the correct FundRef Registry organization names. If a name was not found in the FundRef registry, it may not be the canonical name form, it may be a program name rather than an organization name, or it may be an organization not yet included in FundRef Registry. If you know of another name form or a parent organization name for a "not found" item on this list below, please share that information.

FundRef Name	FundRef Organization Name
Division of Civil, Mechanical and Manufacturing Innovation	Division of Civil, Mechanical and Manufacturing Innovation
Congressionally Directed Medical Research Programs	Congressionally Directed Medical Research Programs
National Institute of Arthritis and Musculoskeletal and Skin Diseases	National Institute of Arthritis and Musculoskeletal and Skin Diseases
National Heart, Lung, and Blood Institute	National Heart, Lung, and Blood Institute
National Cancer Institute	National Cancer Institute
National Institutes of Health	
Department of Defense	
National Science Foundation	National Science Foundation
ARCS Roche Foundation Scholar Award Program	

C. Plunkett, A. Kumar, J. Yrastorza, Y.-H. Hou, J. Placone, G. Grennan, A. J. Engler* 1901366

H-Ras Transformation of Mammary Epithelial Cells Induces ERK-Mediated Spreading on Low Stiffness Matrix

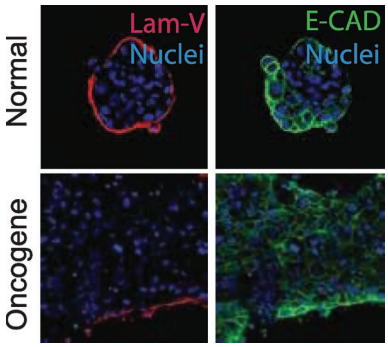

Oncogenes and material stiffness can facilitate the transformation of epithelial cells into mesenchymal cells, a process necessary for tumor formation. Their combined effect on this process, however, is unclear. Cells with and without expression of an oncogene, H-Ras, are cultured on substrates of normal and malignant mammary tissue. The oncogene can dominate mechanical signals from the adjacent material to drive cell transformation independent of material stiffness.

ADVANCED HEALTHCARE MATERIALS
www.advhealthmat.de

H-Ras Transformation of Mammary Epithelial Cells Induces ERK-Mediated Spreading on Low Stiffness Matrix

Christopher Plunkett, Aditya Kumar, Jaime Yrastorza, Yang-Hsun Hou, Jesse Placone, Gillian Grennan, and Adam J. Engler*

Oncogenic transformation of mammary epithelial cells (MECs) is a critical step in epithelial-to-mesenchymal transition (EMT), but evidence also shows that MECs undergo EMT with increasing matrix stiffness; the interplay of genetic and environmental effects on EMT is not clear. To understand their combinatorial effects on EMT, premalignant MCF10A and isogenic Ras-transformed MCF10AT are cultured on polyacrylamide gels ranging from normal mammary stiffness, ≈150 Pa, to tumor stiffness, ≈5700 Pa. Though cells spread on stiff hydrogels independent of transformation, only 10AT cells exhibit heterogeneous spreading behavior on soft hydrogels. Within this mixed population, spread cells exhibit an elongated, mesenchymal-like morphology, disrupted localization of the basement membrane, and nuclear localization of the EMT transcription factor TWIST1. MCF10AT spreading is not driven by typical mechanosensitive pathways including YAP and TGF-β or by myosin contraction. Rather, ERK activation induces spreading of MCF10AT cells on soft hydrogels and requires dynamic microtubules. These findings indicate the importance of oncogenic signals, and their hierarchy with substrate mechanics, in regulating MEC EMT.

1. Introduction

Carcinogenesis is a complex, multistep process that begins with the accumulation of mutations that transforms a healthy cell into a malignant one.[1] Genomic profiling has identified a number of oncogenes that are commonly mutated in tumors, but ascertaining their specific effects can be difficult as any given tumor may have combinations of multiple mutations within and between cells.[2] To reduce the complexity of heterogenous, multivariant tumors, researchers have transformed cells with specific oncogenes to permit their isogenic interrogation.[3] For example, the Ras gene is commonly mutated in breast cancers, inducing increased cell proliferation, migration, and survival,[4] and to more easily examine its function, an H-Ras transformed clone, i.e., 10AT—referred to as 10AT, was created from pre-malignant mammary epithelial cells (MECs), i.e., 10A—referred to as 10A. Subsequently extensive genomic, transcriptomic, and proteomic analyses have been performed on these paired cell lines, identifying several genes, such as c-myc, cyclins, and cell surface receptors, that are upregulated by Ras transformation.[5,6]

One classically defined pathway associated with H-Ras transformation involves the activation of extracellular signal-regulated kinase (ERK).[7] ERK activation has been shown to affect biological processes such as the dysregulation of cell proliferation and apoptosis and increased migratory propensity, thus highlighting the interest in studying this kinase in the cancer community. However, ERK activation appears to be cell and context specific, resulting in differences in downstream signaling and subsequent cell behavior.[8] In 10AT cells, ERK activation alone appears to be insufficient to induce migration and instead requires the additional activation of p38 or Y-box binding protein-1 to induce migration.[9,10] Thus, additional research is needed to understand ERK signaling as well as identification of downstream targets in various context.

The accumulation of genetic alterations is a well-established factor in tumor pathogenesis, although several other factors in the extracellular niche can also drive disease to varying effects. Extensive remodeling of the tumor microenvironment takes place during initiation, growth and metastasis of the tumor as well as its adjacent parenchyma. For example, mammary stroma experiences large increases in extracellular matrix (ECM) proteins, such as collagen and fibronectin, as well as increased crosslinking and fiber alignment, during tumor progression.[11] These changes increase ECM stiffness, which induces depolarization of mammary acini and invasion of MECs into the microenvironment.[12] A variety of potentially redundant mechanisms have been identified, namely epithelial

C. Plunkett, A. Kumar, J. Yrastorza, Y.-H. Hou, J. Placone,[+] G. Grennan, A. J. Engler
Department of Bioengineering
UC San Diego
La Jolla, CA 92093, USA
E-mail: aengler@ucsd.edu
A. J. Engler
Biomedical Sciences Program
UC San Diego
La Jolla, CA 92093, USA
A. J. Engler
Sanford Consortium for Regenerative Medicine
La Jolla, CA 92037, USA
The ORCID identification number(s) for the author(s) of this article can be found under https://doi.org/10.1002/adhm.201901366.
[+]Present address: Department of Physics and Engineering, West Chester University, West Chester, PA 19383, USA

DOI: 10.1002/adhm.201901366

to mesenchymal transition (EMT) through localization of the basic helix loop helix transcription factor Twist1[13] as well as activation of other mechanosensitive proteins such as YAP/TAZ and SMAD 2/3.[14] More recently, 3D culture of MECs on a soft but dynamic hydrogel results in acinar polarization that can be induced later to undergo EMT by stiffening the matrix; such dynamics more accurately models in vivo behavior and dramatic changes in morphology, gene expression, and response to drugs.[14–16] Conversely, in vivo ECM actually softens during therapeutic interventions such as radiation.[17]

Both oncogenic transformation and ECM stiffness contribute to tumor pathogenesis, but as outlined above, each has been largely observed independently of the other. Thus, we sought to understand the interplay of these factors by culturing the 10A cell lines on hydrogels that mimic stiffness ranging from that of healthy to malignant tissue. We hypothesized that as mutation burden increased, sensitivity to mechanical cues would concurrently decrease and lead to increased spreading at lower stiffness. While we specifically investigated the 10A and 10AT lines, this approach can easily be applied to other isogenic cell pairs to better understand this interplay in the context of different oncogenes and cancer types.

2. Results

2.1. H-Ras Transformation Induces Stiffness Insensitivity in Mammary Epithelial Cells

Elevated microenvironment stiffness induces invasive behavior in benign 10A MECs;[12] to determine whether malignant MECs show an altered sensitivity to niche stiffness, we cultured 10A cells and isogenic H-Ras transformed 10AT cells, as well as lines derived from 10AT xenografts, MCF10DCIS and MCF10CA1—referred to as 10DCIS and 10CA1, on polyacrylamide hydrogels ranging from physiologically soft (≈150 Pa) to pathologically stiff (≈5700 Pa) conditions. Typically MECs form large spheroids in 3D cultures or Matrigel overlaid 2D substrates and eventually hollow out with increasing maturity.[12] When substrate stiffness exceeded 670 Pa, all cell lines began to or exhibited complete loss of spheroid morphology and increased spread behavior (Figure S1A, Supporting Information). At or below 670 Pa, only 10AT spheroids exhibited morphologic changes (**Figure 1**A,B and Figure S1A,B, Supporting Information), with fewer spheroids and more spread cells in the surrounding environment compared to 10A cells (Figure 1C,D). While 10A response was largely homogeneous, whether circular or spread, the 10AT response on soft substrates was more heterogeneous owing to higher standard deviations in these metrics.

2.2. H-Ras Transformed Cells Undergo Heterogeneous EMT in a Soft Microenvironment

Cellular invasion of mammary stroma in stiff environmental conditions has been associated with an EMT transition whereby invading cells lose junction and basement membrane stability and adopt an elongated morphology.[18] To explore whether the spread 10AT cell population on soft hydrogels undergo aspects

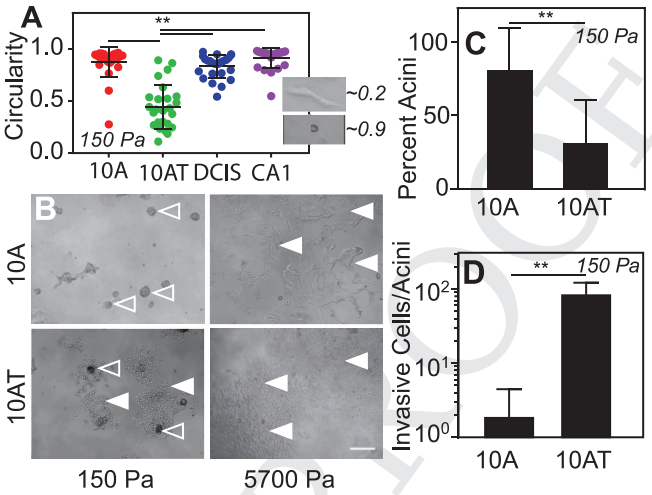

Figure 1. H-Ras transformed cells show heterogeneous spread behavior at physiologically soft mammary stiffness. A) Cell circularity for MECs on soft substrates. Inset demonstrates the circularity of different morphologies. $^{**}p < 0.01$, ANOVA with Tukey's post hoc analysis. $n = 3$. B) Bright-field images of MECs cultured on soft and stiff PA substrates. Hollow arrows indicated acini while solid arrows indicate spread regions. Scale bar is 250 µm. C) Total percentage of acini present per hydrogel on soft substrates for each MEC line. $^{**}p < 0.01$, unpaired t-test with Welch's correction. $n = 3$. D) Average number of spread cells produced per acini on soft substrates. $^{**}p < 0.01$, unpaired t-test with Welch's correction. $n = 3$.

of EMT, we examined E-Cadherin and Laminin V expression on soft and stiff hydrogels to observe junctions and basement membrane, respectively. Whereas all cell lines showed a loss of Laminin V on stiff hydrogels (**Figure 2**A and Figure S2A, Supporting Information), only 10AT cells had destabilized basement membranes on all substrates (Figure 2A and Figure S2A, Supporting Information). To further explore the upstream EMT activators, we measured mRNA expression of five key transcription factors associated with EMT, Snail, Slug, Zeb1, Zeb2, and Twist1. This showed no significant differences in expression levels between groups (Figure S2B, Supporting Information), although it has been noted that transcriptional activity of some markers requires nuclear localization.[13,14] Thus we documented localization changes of Twist1, finding that in stiff conditions, it became nuclear localized for all cell lines (Figure 2B,C and Figure S2C, Supporting Information). However, for cells on soft substrates, 10AT was the only line to indicate Twist1 localization, albeit with remnants of spheroids exhibiting significant cytoplasmic Twist1 (Figure 2B,C). These data suggest that TWIST localization is not being driven by ECM stiffness in this context, so we examined other signaling molecules associated with the induction of EMT that have previously been implicated in mechanotransduction.[14,19,20] No increase in TGF-β mediated SMAD2/3 localization was detected within spread regions and TGF-β inhibition via Galunisertib did not prevent cells from spreading (Figure S3A, Supporting Information). Likewise, treatment with the YAP inhibitor Verteporfin did not prevent spreading (Figure S3B, Supporting Information). Thus, unlike in benign MECs, our data suggests that the spread subpopulation of H-Ras transformed cells exhibit EMT behavior on soft substrates via oncogene specific activation.

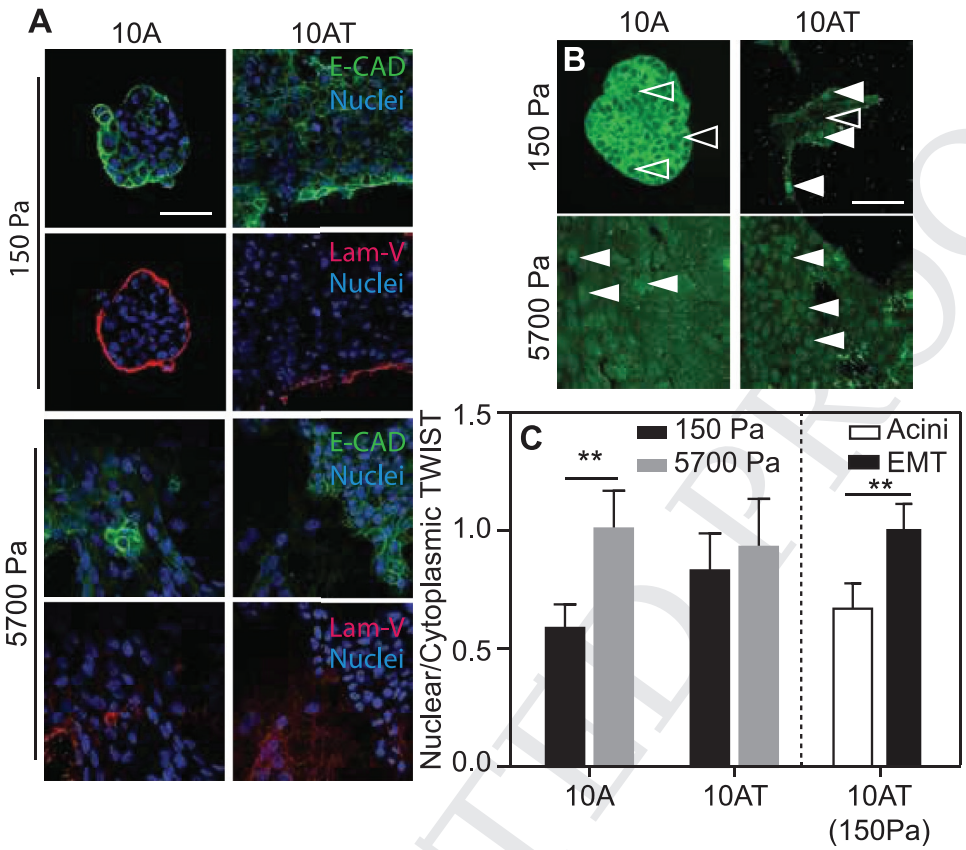

Figure 2. Spread subpopulations of H-Ras transformed cells undergo EMT on soft substrates. A) Immunofluorescent staining for E-Cadherin (green), Laminin V (red), and DAPI (blue). Scale bar is 50 µm. B) Immunofluorescent staining of TWIST1 where hollow arrows indicate non-nuclear localizing transcription factor while solid arrows indicate localized transcription factor. Scale bar is 50 µm. C) TWIST nuclear-to-cytoplasmic fluorescent intensity ratio. Right black and white bars show the ratio for 10AT cells in acinar (left bar) or mesenchymal-like structures (right bar) on soft hydrogels. $^{**}p < 0.01$, nonpaired *t*-test with Welch's correction. $n = 3$.

2.3. H-Ras Spreading in a Soft Microenvironment is Predicated upon ERK Signaling and Microtubule Dynamics

Given the suggestion that H-Ras-mediated spreading is non-mechanotransductive, we next interrogated classic Ras pathway components, e.g., ERK activation,[7] to understand the effects in soft matrices. Whereas ERK activation increased for 10A cells cultured on stiff gels compared to those on soft, ERK was activated at far higher levels for 10AT cells regardless of stiffness (**Figure 3**A,B). With high ERK activation independent of stiffness, we next determined whether 10AT spreading is ERK-dependent; cells were treated with the ERK inhibitor SCH772984 immediately upon or four days after seeding. On stiff substrates, ERK inhibition had no effect on cell spreading for either line (Figure 3C and Figure S4A–C, Supporting Information), which is consistent with activation of EMT-associated, mechanosensitive proteins. ERK inhibition dramatically reduced spreading of 10AT cells on soft conditions, but only when the drug was added from the outset (Figure 3C). To understand the downstream effects of ERK activation on the cytoskeletal organization—which regulates spreading, we treated cells with the microtubule inhibitors nocodazole (tubulin-binding) and paclitaxel (microtubule capping) and the myosin inhibitor blebbistatin. Microtubule remodeling inhibitors prevented 10AT cell spreading on soft substrates but induced a heterogeneous response for both 10A and 10AT cells on stiff substrates; a subset of the cells rounded up while the remaining cells spread (Figure 3D and Figure S4D–G, Supporting Information). No reduction in spreading was observed with blebbistatin, suggesting that actomyosin contraction is less involved in H-Ras- or stiffness-mediate cytoskeleton remodeling in MECs undergoing EMT (Figure 3D and Figure S4D–G, Supporting Information). Together these data imply an indirect pathway between H-Ras and MEK that turns on ERK phosphorylation and leads to changes in microtubule dynamics in a stiffness-independent manner (**Figure 4**).

3. Discussion

Understanding how oncogenes contribute to carcinogenesis is difficult due the inherent heterogeneity of tumors in vivo.[1,2] Oncogenic transformation of healthy cells has served as a powerful tool to understand mechanisms,[3] but since all cells sense their environment, it is important to understand to what extent stiffness can mediate EMT in the presence of an oncogene.[12–14,19] To illustrate this point, we demonstrated that H-Ras transformed MECs are insensitive to stiffness and adopt

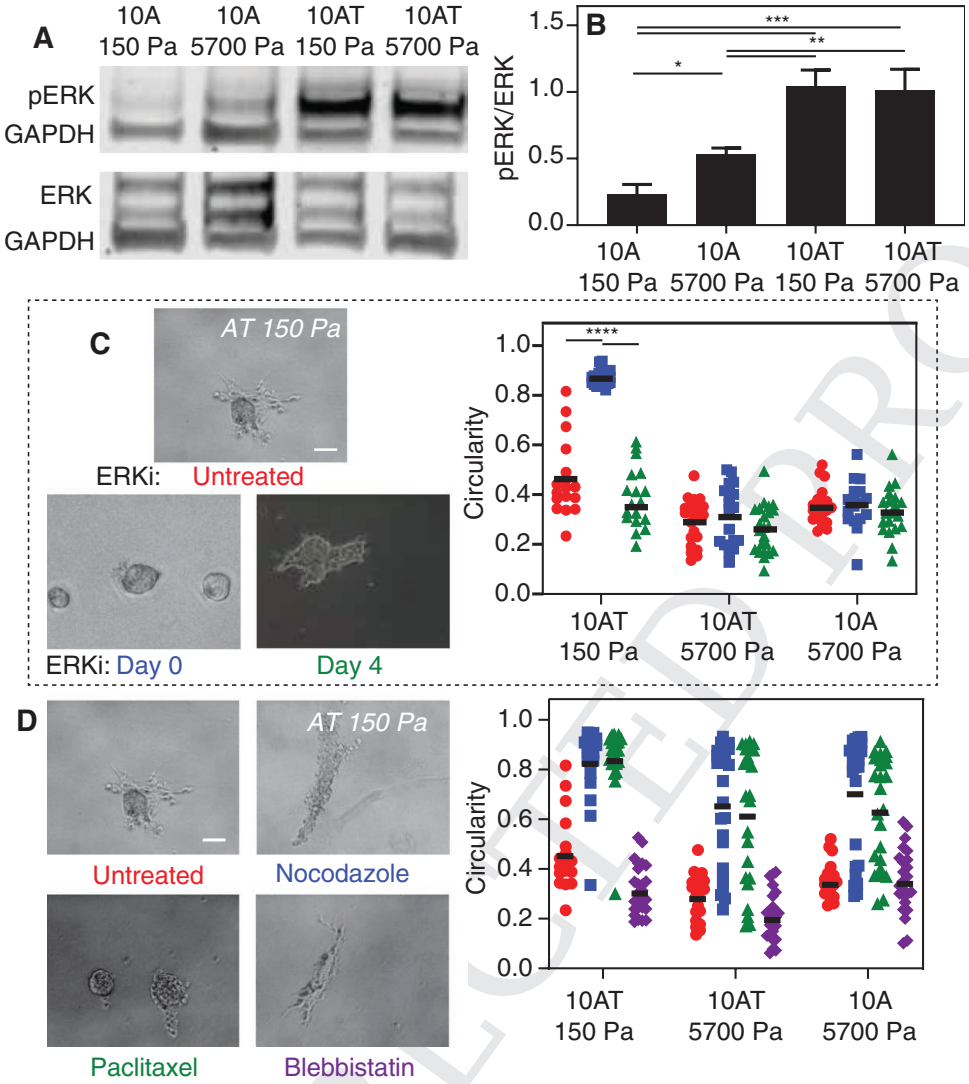

Figure 3. H-Ras Induces ERK-Mediated Spreading Via Microtubule Polymerization. A) Western blots showing phosphorylated and total ERK expression for cell lines on different stiffness. Values were normalized to GAPDH expression as a loading control and plotted in panel (B). $*p < 0.05$, $*p < 0.01$, $***p < 0.001$, ANOVA with Tukey's post hoc analysis. $n = 3$. C) Brightfield images of 10AT spheroids on soft substrates that are either untreated or treated with ERK inhibitor at the time of seeding or after four days of culture. Cell circularity for lines on different stiffness and drug timing are plotted with a bar representing the mean. $****p < 0.0001$, ANOVA with Tukey's post hoc analysis. $n = 3$. Scale bar 100 µm. D) Brightfield images of 10AT spheroids on soft substrates that are either untreated or treated with microtubule and myosin inhibitors and cell circularity for cell lines on different stiffness and drugs. Scale bar 100 µm.

a partially spread phenotype on substrates with physiologically healthy stiffness. This spread cell fraction underwent EMT, allowing for increased migratory capacity via ERK-mediated microtubule dynamics.

Although H-Ras activation of ERK and subsequent microtubule polymerization has been demonstrated before,[21] this is the first study to demonstrate that ERK inhibition is sufficient to prevent H-Ras induced cell spreading on soft matrix. Interestingly, previous studies using H-Ras transformed 10A cells demonstrated that whereas p38 activation was sufficient to induce cell invasion in a transwell model,[10,22] ERK activation was not. These data highlight how specific matrix conditions, i.e., cell confinement during migration through a pore versus matrix stiffness, can induce different signaling pathways in transformed cell lines, which ultimately lead to nearly identical behaviors including cell spreading and migration. Interestingly and unlike with other extracellular signals, we found distinct subpopulations of H-Ras transformed cells that were or were not responsive to substrate stiffness, i.e., clustered or spread on soft substrates. Such heterogeneity is consistent with tumor behavior in patients and when cells are cultured on dynamic substrates where the specific amount of several signaling pathways could dictate more or less spheroid formation.[14] However observing heterogeneous responses within the 10AT line suggests some stochasticity in mechanotransduction pathways not directly assessed here. Aside from spreading, cytoskeletal remodeling downstream of ERK was also heterogeneous; application of microtubule inhibitors on soft matrix reduced 10AT

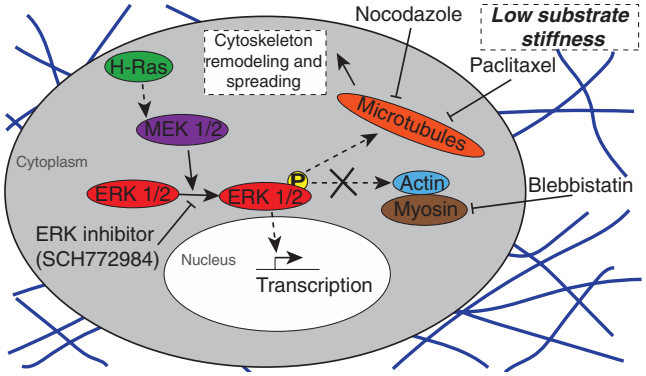

Figure 4. Schematic of 10AT signaling on low stiffness substrates. Unlike on stiff substrates where cells mechanosense, active H-Ras signaling on soft substrates in 10AT cells leads to downstream activation of MEK 1/2 and subsequently ERK 1/2 phosphorylation. Downstream targets of ERK 1/2 are implicated in cell proliferation, cytoskeleton rearrangement, and preventing cell death. Inhibition of ERK phosphorylation prevents spreading on low stiffness substrates. Downstream of ERK, cytoskeletal assembly, which impacts cell spreading, is differentially responsive: inhibition of microtubule dynamics via nocodazole and paclitaxel, but not actomyosin dynamics with blebbistatin, prevents spreading of H-Ras transformed cells.

spreading but was less effective for both lines on stiff matrix. These data imply that H-Ras-mediated spreading was blocked on soft substrates but that stiffness-mediated spreading was only partially blocked on stiff substrates. While previously observed,[23] i.e., that there are overlapping mechanosensitive pathways,[14] these data highlight the importance of considering culture conditions in cell response. Given that even different RAS mutations can play different roles in cancer initiation compared to cancer progression,[24] observing how cells respond across the stiffness spectrum of cancer can provide insight into specific oncogene function.

4. Conclusions

These findings suggest that as tumors continue to develop and accumulate oncogenic mutation, the sensitivity of malignant cells may drive premature spreading behavior. It is therefore of great importance to identify and explore the role of other key mammary cell mutations such as BRCA1, B-RAF, or PI3K in altering stiffness sensitivity. These mutations may, through a similar mechanism, sensitize tumor masses to stiffness to differing degrees to permit destabilization of tumor spheroids and spreading.

5. Experimental Section

Cell Culture: MCF10A and MCF10AT cells (referred to as 10A and 10AT, respectively) were expanded in ~~DMEM~~/F12 media containing 5% horse serum, 20 ng mL^{-1} human EGF, 0.5 µg mL^{-1} hydrocortisone, 100 ng mL^{-1} cholera toxin, 10 µg mL^{-1} insulin, and 1% penicillin and streptomycin (Sigma-Aldrich). MCF10DCIS and MCF10CA1 were expanded in DMEM/F12 media containing 5% horse serum and 1% penicillin and streptomycin. Cells were detached when they reached 80% confluency using 0.05% trypsin for 7 min. Trypsin was neutralized using DMEM/F12 media containing 20% horse serum and cells were split 1:5 and reseeded. Cells were only used up to passage 10.

Polyacrylamide Hydrogel Synthesis: Polyacrylamide gels were prepared as previously described.[25] 12 mm glass coverslips were methacrylated by first treating with UV-Ozone (BioForce Nanosciences) for 5 min followed by functionalization with 20 × 10^{-3} M 3-(trimethoxysilyl) propyl methacrylate (Sigma-Aldrich) for 5 min. Hydrogel solutions were prepared by mixing acrylamide/bis-acrylamide solutions (Fisher) with 1% v/v of 10% ammonium persulfate (Fisher) and 0.1% v/v of *N*,*N*,*N*′,*N*′,-tetramethylethylenediamine (VWR International). 3%/0.3%, 4%/0.3%, 3%/0.6%, and 5%/0.15% acrylamide/bis-acrylamide concentrations were used to achieve stiffness of 150, 320, 670, and 5700 Pa, respectively. 15 µL of solution was sandwiched between a functionalized coverslip and a dichlorodimethylsilane (Acros Organics)-coated glass slide. Polymerized gels were then washed with phosphate-buffered saline (PBS) and incubated with 0.2 mg mL^{-1} Sulfo-SANPAH in 50 × 10^{-3} M ~~HEPES~~ pH 8.5 in the presence of 350 nm UV light (4 mW cm^{-2}, UVP) for 10 min, rinsed twice with PBS, and incubated overnight at 37 °C with 0.15 mg mL^{-1} rat tail Collagen I (Millipore) in PBS. Gels were then rinsed with PBS and UV sterilized at 254 nm for 2 h at prior to use. Q3

3D Cell Culture: Cells were seeded on hydrogels in the presence of 2% Matrigel (Corning) mixed with DMEM/F12 supplemented with 2% horse serum, 5 ng mL^{-1} human EGF, 0.5 mg mL^{-1} hydrocortisone, 100 ng mL^{-1} cholera toxin, 10 µg mL^{-1} insulin, and 1% penicillin and streptomycin. Cells were seeded on hydrogels at a density of 2000 cells per gel and allowed six days in culture to form mammary organoids. For drug experiments, cells were treated with SCH772984 (0.1 × 10^{-6}–10 × 10^{-6} M) either upon seeding or after 4 days of culture on hydrogels. Cells were dosed with nocodazole (0.05–2 µg mL^{-1}), paclitaxel (0.5–1 µg mL^{-1}), and blebbistatin (5 × 10^{-6}–50 × 10^{-6} M). Images were taken in 10× brightfield on day 6.

3D Cell Culture—Morphological Analysis: Brightfield images were acquired on a Nikon Eclipse Ti-S inverted microscope with a 10× objective and analyzed in ImageJ. Circularity was calculated by tracing cell boundaries and applying the following equation: Circularity = 4π(area/perimeter)^2. Percent acini was calculated by categorizing cells as either acinar or spread based on circularity and determining how many acinar regions remained. Spread cells per acini was calculated by counting the number of cells that migrated away from a specific acinus.

Immunofluorescence: Cells were fixed with 3.7% formaldehyde for 15 min at room temperature. Matrigel was removed from samples by incubation in 5 × 10^{-3} M ~~EDTA~~ (Fisher) for 30 min at 4 °C. Samples were then permeabilized with PBS supplemented with $MgCl_2$ (final concentration 0.5 × 10^{-3} M) (Solution A) and 0.5% Triton X-100 for 15 min at room temperature. Sample blocking was performed in a solution of 20% goat serum and 0.2% Triton-X 100 in Solution A for 30 min at room temperature. Primary antibodies were added and incubated overnight at 4 °C. Dilutions were as follows: Anti-E-Cadherin (BD, cat # 610181, 1:50), Laminin V (abcam, cat # ab11575, 1:100), TWIST1 (Santa Cruz Biotechnology, cat # sc-81417, 1:25), and SMAD2/3 (Cell Signaling Technology, cat # D7G7, 1:1600). Samples were washed three times with Solution A for 5 min and subsequently incubated in secondary antibody solution (0.2% TritonX-100 and 20% Goat Serum in Solution A) at the following dilutions: Goat antimouse 488 (Invitrogen, A11004, lot 1218263, 1:500), Goat antirabbit 568 (A11011, Lot 1345045, 1:500) for 1 h at room temperature. Samples were again washed three times for 5 min with Solution A and nuclei were counterstained with DAPI (Thermo, cat # D1306, 1:5000) in dH2O for 3 min. Hydrogels were mounted to glass slides using Fluoromount-G (Southern Biotech, cat # 0100-01) and allowed to dry for 1 h after which gels were sealed with nail polish. Confocal images were taken on a Zeiss LSM 780 with a 40× water immersion objective.

For TWIST analysis, images were linearly analyzed in ImageJ and Zen software packages. Nuclear to cytoplasmic intensity ratios were calculated by first measuring the average nuclear fluorescent intensity for an individual cell and subsequently normalizing it to the same cell's average cytoplasmic fluorescent intensity. This process was carried

out in both "Acini" and "EMT" regions as determined by the software operator for 10AT cells on soft substrates.

Western Blotting: Western blot analysis was performed as described.[26] Briefly, cells were cultured on hydrogels for 6 days before lysis using RIPA buffer (50×10^{-3} M HEPES, 150×10^{-3} M NaCl, 1.5×10^{-3} M $MgCl_2$, 1×10^{-3} M EDTA, 1% Triton, 10% glycerol, 25×10^{-3} M sodium deoxycholate, 0.1% SDS) containing Roche Complete Protease Inhibitor (Sigma-Aldrich) and PhosSTOP (Sigma-Aldrich). Protein concentrations of the samples were determined using a Pierce BCA Protein Assay kit (Thermo Scientific). 10 µg of protein from each sample was loaded into Bolt 4–12% Bis–Tris gels (Thermo) and separated by electrophoresis in ~~MES~~ running buffer (50×10^{-3} M ~~MES~~, 50×10^{-3} M Tris Base, 1×10^{-3} M EDTA, 0.1% w/v SDS) under reducing and denaturing conditions before being transferred onto a nitrocellulose membrane using the iBlot 1 semidry transfer system (Invitrogen). Membranes were incubated with 5% Seablock blocking buffer (Thermo) in Tris buffered saline with tween (150×10^{-3} M NaCl, 15×10^{-3} M Tris–HCl, 20×10^{-3} M Tris Base, 0.1% Tween) for 1 h followed by overnight incubation with either phosphorylated ERK (1:1000, Cell Signaling, cat # 9101) or total ERK (1:1000, Cell Signaling, cat # 9102) and Glyceraldehyde 3-phosphate dehydrogenase (1:7500 Abcam, cat # ab9484). Membranes were then incubated with Alexa Fluor 680 donkey anti-mouse (0.2 µg mL^{-1}, Thermo, cat # A10038) and Alexa Fluor 790 donkey antirabbit (0.2 µg mL^{-1}, Thermo, cat # A11374) for 2 h. Blots were imaged using the Li-Cor Odyssey CLx imaging system (Li-Cor) and the integrated densities of bands were analyzed using the Li-Cor Image Studio Lite software.

Quantitative PCR: To separate acini and spread cell regions, gels were mechanically dissected using a Zeiss Stereo Discovery. V8 for visualization. Resection of organoids was performed using a microdissection scalpel. Spread cell regions were then exposed to 0.05% Trypsin for 5 min to lift cells off the gels. RNA was isolated from these samples using Trizol-chloroform extraction per manufacturer's instructions (Thermo Fisher Scientific). cDNA was synthesized using 2 µg RNA and SuperScript III reverse transcriptase (Thermo Fisher Scientific) with random hexamer primers. Quantification (45 cycles, 95 °C for 15 s followed by 60 °C for 1 min) was carried out on a CFX384 Touch RT-PCR system (BioRad) with a SYBR Green probe (Thermo Fisher Scientific). Data were analyzed based on a standard curve generated from a fibronectin plasmid and all samples were normalized to GAPDH. Primers are listed in Table S1 (Supporting Information).

Statistics: Statistical significance was determined using a Student's *t*-test with Welch's correction or ANOVA with Tukey's post hoc analysis as denoted. Analysis was performed using Graphpad Prism software, with the threshold for significance level set at $p < 0.05$. All data are presented as mean ± standard deviation.

Supporting Information

Supporting Information is available from the Wiley Online Library or from the author.

Acknowledgements

Funding for this work was provided by National Institutes of Health grants R01CA206880 (A.J.E.), R21CA217735 (A.J.E.), F32HL126406 (J.K.P.), and T32AR060712 (A.K.), Department of Defense grant W81XWH-13-1-0133 (A.J.E.), National Science Foundation grants 1463689 (A.J.E.) and 1763139 (A.J.E.) and the Graduate Research Fellowship program (A.K.), and the ARCS/Roche Foundation Scholar Award Program in the Life Science (A.K.).

Conflict of Interest

The authors declare no conflict of interest.

Author Contributions

C.M.P., A.K., and A.J.E. conceived of the project and designed the experiments. C.M.P., A.K., J.Y., Y.H., G.G., and J.K.P. performed all cell assays. The manuscript was written by C.M.P., A.K., and A.J.E. with input from the other authors.

Keywords

breast cancer, gene-material interactions, H-ras, matrix stiffness, microtubules

Received: September 26, 2019
Revised: November 27, 2019
Published online:

[1] R. E. Scott, J. J. Wille, M. L. Wier, *Mayo Clin. Proc.* **1984**, *59*, 107.
[2] F. Di Nicolantonio, S. Arena, M. Gallicchio, A. Bardelli, *Cell Cycle* **2010**, *9*, 20.
[3] B. Elenbaas, L. Spirio, F. Koerner, M. D. Fleming, D. B. Zimonjic, J. L. Donaher, N. C. Popescu, W. C. Hahn, R. A. Weinberg, *Genes Dev.* **2001**, *15*, 50.
[4] J. J. Zhao, O. V. Gjoerup, R. R. Subramanian, Y. Cheng, W. Chen, T. M. Roberts, W. C. Hahn, *Cancer Cell* **2003**, *3*, 483.
[5] J. Y. So, H. J. Lee, P. Kramata, A. Minden, N. Suh, *Mol. Cell Pharmacol.* **2012**, *4*, 31.
[6] S. L. Maguire, B. Peck, P. T. Wai, J. Campbell, H. Barker, A. Gulati, F. Daley, S. Vyse, P. Huang, C. J. Lord, G. Farnie, K. Brennan, R. Natrajan, *J. Pathol.* **2016**, *240*, 315.
[7] F. Liu, X. Yang, M. Geng, M. Huang, *Acta Pharm. Sin. B* **2018**, *8*, 552.
[8] P. J. Roberts, C. J. Der, *Oncogene* **2007**, *26*, 3291.
[9] V. Evdokimova, C. Tognon, T. Ng, P. Ruzanov, N. Melnyk, D. Fink, A. Sorokin, L. P. Ovchinnikov, E. Davicioni, T. J. Triche, P. H. B. Sorensen, *Cancer Cell* **2009**, *15*, 402.
[10] M. S. Kim, E. J. Lee, H. R. C. Kim, A. Moon, *Cancer Res.* **2003**, *63*, 5454.
[11] M. W. Conklin, J. C. Eickhoff, K. M. Riching, C. A. Pehlke, K. W. Eliceiri, P. P. Provenzano, A. Friedl, P. J. Keely, *Am. J. Pathol.* **2011**, *178*, 1221.
[12] M. J. Paszek, N. Zahir, K. R. Johnson, J. N. Lakins, G. I. Rozenberg, A. Gefen, C. A. Reinhart-King, S. S. Margulies, M. Dembo, D. Boettiger, D. A. Hammer, V. M. Weaver, *Cancer Cell* **2005**, *8*, 241.
[13] S. C. Wei, L. Fattet, J. H. Tsai, Y. Guo, V. H. Pai, H. E. Majeski, A. C. Chen, R. L. Sah, S. S. Taylor, A. J. Engler, J. Yang, *Nat. Cell Biol.* **2015**, *17*, 678.
[14] M. G. Ondeck, A. Kumar, J. K. Placone, C. M. Plunkett, B. F. Matte, K. C. Wong, L. Fattet, J. Yang, A. J. Engler, *Proc. Natl. Acad. Sci. USA* **2019**, *116*, 3502.
[15] P. A. Kenny, G. Y. Lee, C. A. Myers, R. M. Neve, J. R. Semeiks, P. T. Spellman, K. Lorenz, E. H. Lee, M. H. Barcellos-Hoff, O. W. Petersen, J. W. Gray, M. J. Bissell, *Mol. Oncol.* **2007**, *1*, 84.
[16] E. J. Haagensen, H. D. Thomas, C. Mudd, E. Tsonou, C. M. Wiggins, R. J. Maxwell, J. D. Moore, D. R. Newell, *Eur. J. Cancer* **2016**, *56*, 69.
[17] J. P. Miller, B. H. Borde, F. Bordeleau, M. R. Zanotelli, D. J. LaValley, D. J. Parker, L. J. Bonassar, S. C. Pannullo, C. A. Reinhart-King, *APL Bioeng.* **2018**, *2*, 031901.
[18] S. Lamouille, J. Xu, R. Derynck, *Nat. Rev. Mol. Cell Biol.* **2014**, *15*, 178.

[19] S. Dupont, L. Morsut, M. Aragona, E. Enzo, S. Giulitti, M. Cordenonsi, F. Zanconato, J. Le Digabel, M. Forcato, S. Bicciato, N. Elvassore, S. Piccolo, *Nature* **2011**, *474*, 179.
[20] Z. Meng, Y. Qiu, K. C. Lin, A. Kumar, J. K. Placone, C. Fang, K.-C. Wang, S. Lu, M. Pan, A. W. Hong, T. Moroishi, M. Luo, S. W. Plouffe, Y. Diao, Z. Ye, H. W. Park, X. Wang, F.-X. Yu, S. Chien, C.-Y. Wang, B. Ren, A. J. Engler, K.-L. Guan, *Nature* **2018**, *560*, 655.
[21] R. E. Harrison, E. A. Turley, *Neoplasia* **2001**, *3*, 385.
[22] I. Shin, S. Kim, H. Song, H. R. C. Kim, A. Moon, *J. Biol. Chem.* **2005**, *280*, 14675.
[23] A. J. Rice, E. Cortes, D. Lachowski, B. C. H. Cheung, S. A. Karim, J. P. Morton, A. Del Río Hernández, *Oncogenesis* **2017**, *6*, e352.
[24] M. S. Miller, L. D. Miller, *Front. Genet.* **2012**, *2*, 1.
[25] B. F. Matte, A. Kumar, J. K. Placone, V. G. Zanella, M. D. Martins, A. J. Engler, M. L. Lamers, *J. Cell Sci.* **2019**, *132*, jcs224360.
[26] A. Kumar, S. K. Thomas, K. C. Wong, V. Lo Sardo, D. S. Cheah, Y.-H. Hou, J. K. Placone, K. P. Tenerelli, W. C. Ferguson, A. Torkamani, E. J. Topol, K. K. Baldwin, A. J. Engler, *Nat. Biomed. Eng.* **2019**, *3*, 137.

ADVANCED HEALTHCARE MATERIALS

Reprint Order Form 2019
- please return with your proofs -

Editorial Office:

Wiley-VCH Verlag, Boschstrasse 12
69469 Weinheim, Germany

Tel.: (+49) 6201 606 235
Fax: (+49) 6201 606 500

E-mail: advhealthmat@wiley-vch.de
http://www.advhealthmat.de

Manuscript No. _____

Please send me and bill me for

☐ no. of **reprints** via ☐ airmail (+ 25 Euro) ☐ surface mail

☐ **high-resolution PDF file** (330 Euro).

My e-mail address:

_____

Please note: It is not permitted to present the PDF file on the internet or on company homepages

★**Special Offer**★ If you order 200 or more reprints you will get a PDF file for half price.

Information regarding VAT
Please note that from German sales tax point of view, the charge for **Reprints, Issues or Posters** is considered as **"supply of goods"** and therefore, in general, such delivery is a subject to German sales tax. However,this regulation has no impact on customers located outside of the European Union. Deliveries to customers outside the Community are automatically tax-exempt. Deliveries within the Community to institutional customers outside of Germany are exempted from the German tax (VAT) only if the customer provides the supplier with his/her VAT number. The VAT number (value added tax identification number) is a tax registration number used in the countries of the European Union to identify corporate entities doing business there. It starts with a country code (e.g. FR for France, GB for Great Britain) and follows by numbers.

Cover Posters

Posters are available of all the published covers and frontispieces in two sizes

☐ DIN A2 42 x 60 cm/ 17 x 24in (one copy: **39 Euro**)

☐ DIN A1 60 x 84 cm/ 24 x 33in (one copy: **49 Euro**)

Postage for shipping posters overseas by airmail:
+ 25 Euro

Postage for shipping posters within Europe by surface mail:
+ 15 Euro

Mail reprints / cover posters to:

_____
_____
_____
_____
_____

Invoice address:

_____
_____
_____
_____
_____

Date, Signature **Stamp**

VAT no.: _____
(institutes / companies in EU countries only)

Purchase Order No.: _____

Credit Card Payment

VISA, MasterCard, AMERICAN EXPRESS
Please use the Credit Card Token Generator located at the website below to create a token for secure payment. The token will be used instead of your credit card number.

Credit Card Token Generator:
https://www.wiley-vch.de/editorial_production/index.php

Please transfer your token number to the space below.

Credit Card Token Number:

Price list for reprints (The prices include mailing and handling charges. All Wiley-VCH prices are exclusive of VAT)

No. of pages	Price (in Euro) for orders of 50 copies	100 copies	150 copies	200 copies	300 copies	500 copies
1-4	345	395	425	445	548	752
5-8	490	573	608	636	784	1077
9-12	640	739	786	824	1016	1396
13-16	780	900	958	1004	1237	1701
17-20	930	1070	1138	1196	1489	2022
for every additional 4 pages	147	169	175	188	231	315

★ **Special Offer** ★ If you order 200 or more reprints you will get a PDF file for half price.

Wiley-VCH Verlag GmbH & Co. KGaA; Location of the Company: Weinheim;
Chairman of the Supervisory Board: John Kritzmacher,
Trade Register: Mannheim, HRB 432833, General Partner: John Wiley & Sons GmbH,
Location: Weinheim, Trade Register Mannheim, HRB 432296,
Managing Directors: Sabine Steinbach, Dr. Guido F. Herrmann

WILEY-VCH